ОБЪЕДИНЕННЫЙ
ИНСТИТУТ
ЯДЕРНЫХ
ИССЛЕДОВАНИЙ

Дубна

E4-99-260

V.K.Lukyanov, E.V.Zemlyanaya

EIKONAL PHASE FOR THE SYMMETRIZED WOODS-SAXON POTENTIAL AND ITS USE FOR HEAVY ION SCATTERING

Submitted to «Journal of Physics»

1999

Лукьянов В.К., Земляная Е.В. E4-99-260

Эйкональная фаза для симметризованного потенциала Вудса — Саксона и ее использование в задачах рассеяния тяжелых ионов

Получено приближенное аналитическое выражение эйкональной фазы для потенциала в виде симметризованной функции Ферми, которое затем проверено сравнениями с точными численными расчетами. Показано, что его можно с успехом применять для ядро-ядерного рассеяния при промежуточных энергиях в десятки МэВ на нуклон в рамках приближения Глаубера — Ситенко для малых углов. На практике использование такой аналитической фазы позволяет понять механизм рассеяния и ускорить примерно на два порядка численный расчет дифференциальных сечений.

Работа выполнена в Лаборатории теоретической физики им.Н.Н.Боголюбова ОИЯИ.

Препринт Объединенного института ядерных исследований. Дубна, 1999

Lukyanov V.K., Zemlyanaya E.V. E4-99-260

Eikonal Phase for the Symmetrized Woods — Saxon Potential and Its Use for Heavy Ion Scattering

An approximate analytic expression of the eikonal phase for the potential in the form of the symmetrized Fermi function is derived and compared with the results of exact calculations. It is shown that this expression can be successfully applied to the intermediate energy nucleus-nucleus scattering of tens of MeV/nucleon in the framework of a Glauber — Sitenko approach at small angles. In practice, the use of the analytic phase permits one to understand a mechanism of scattering and calculate differential cross sections about two orders faster than with the whole numerical integration.

The investigation has been performed at the Bogoliubov Laboratory of Theoretical Physics, JINR.

Preprint of the Joint Institute for Nuclear Research. Dubna, 1999

1 Introduction

The high-energy methods, applied to scattering problems at $E \gg U$ and $kR \gg 1$, have been improved mainly for studying hadron- and light- ion collisions with nuclei, and many calculations were fulfilled in the framework of the Glauber-Sitenko approach to small angles [1], [2] by numerical integrations of the elastic scattering amplitude

$$f(q) = ik \int_0^\infty db\, bJ_0(qb)\,(1 - e^{i\Phi_N + i\Phi_C}), \qquad q < \sqrt{2k/R}, \tag{1.1}$$

and the reaction cross section

$$\sigma_R = 2\pi \int_0^\infty db\, b\,(1 - e^{-2Im\ \Phi_N}). \tag{1.2}$$

Here b and $q = 2k\sin(\theta/2)$ are the impact parameter and transfer momentum, the last being connected with the scattering angle θ. The Coulomb and nuclear eikonal phases $\Phi_C(b)$ and $\Phi_N(b)$ (eikonals) are given as

$$\Phi = -\frac{1}{\hbar v}\int_{-\infty}^{\infty} dz\ U(\sqrt{b^2+z^2}) = -\frac{U_0}{\hbar v} I(b), \tag{1.3}$$

where the thickness function (or profile integral)

$$I(b) = \int_{-\infty}^{\infty} dz\ u(\sqrt{b^2+z^2}) \tag{1.4}$$

depends of the distribution function $u(r)$ of a potential $U(r) = U_0\,u(r)$.

As to heavy ion collisions, they are characterized by extended nuclear potentials of the large radii $R = R_1 + R_2$ and the strong Coulomb fields having long tails. So, large distances of integration require much time for numerical calculations. Moreover, when $kR \gg 1$, the obtained results occur to be very sensitive to precise behaviour of potentials and eikonal phases Φ in the periphery of collisions. Then, to compute the amplitude (1.1) and cross section (1.2), preliminary integration (1.3) over z should be performed many times to obtain eikonals for a set of b. Thus, to make clear the physics of processes and achieve faster computations, it is desirable to get phases in an analytic form. In [1], they were obtained explicitly for the point Coulomb, Gaussian and uniform distributions of a

potential. However, when exploring heavy ion collisions, a shape of the realistic nuclear Woods-Saxon potential and charge and matter density distributions are usually associated with the Fermi function

$$u_F(r) = \frac{1}{1 + \exp[(r-R)/a]} \tag{1.5}$$

or somewhat like that. Below, we use the symmetrized form of (1.5) [3], [4] (SF-function), having certain advantages from both physical and mathematical point of view (see, e.g., [5], [6]), which can be written as

$$u_{SF}(r) = \frac{\sinh(R/a)}{\cosh(R/a) + \cosh(r/a)} = u_F(r) - \delta(r), \tag{1.6}$$

where

$$\delta(r) = \frac{\exp(-R/a)}{\exp(r/a) + \exp(-R/a)}. \tag{1.7}$$

It is seen that, in numerical calculations, the additional term $\delta(r)$ may be neglected for $R \gg a$ when $\exp(-R/a) \ll 1$, and, therefore, $u_F(r)$ and $u_{SF}(r)$ have almost the same form for $r \geq 0$. However, δ plays an important role in the case of comparable R and a. Indeed, in this case the non-physical "cusp" of u_F at $r = 0$ (i.e. $u'(0) \neq 0$) becomes very appreciable, whereas u_{SF} assures that its derivative $u'_{SF}(r=0)$ is equal to zero at any R and a. Moreover, when developing analytical methods of estimations of amplitudes, the use of u_{SF} permits one to exclude many mathematical problems arising in the case of the Fermi function.

The purpose of this work is to obtain an appropriate analytic expression for the nuclear profile function in the case of SF-distribution

$$I(b) = \int_{-\infty}^{\infty} dz\ \frac{\sinh(R/a)}{\cosh(R/a) + \cosh(\sqrt{b^2+z^2}/a)}, \tag{1.8}$$

and test its applicability to the intermediate energy nucleus-nucleus scattering.

Unfortunately, this type of integrals is not suitable for analytic estimations. The only example has been given in [7] where, for the Fermi function, $I_F(b)$ was presented as an infinite series of residues at poles of its integrand. However, it turned out that too many terms are required to provide necessary precision at large b, where the profile integral must fall down as an exponential function.

2 Profile integral for the SF-function

In order to estimate the integral (1.8) we first transform it to that having dependence on only one parameter $C = R/a$ instead of two, the radius R and diffuseness a. To this end we introduce variables $\zeta = z/a$ and $\beta = b/R$ and obtain

$$I(b) \equiv I(\beta R) = 2RI(\beta), \tag{2.1}$$

where

$$\mathcal{I}(\beta) = \frac{1}{C}\int_0^\infty \frac{\sinh C\, d\zeta}{\cosh C + \cosh\sqrt{(\beta C)^2+\zeta^2}}. \qquad (2.2)$$

For further simplifications, it is desirable to transform the denominator to the form which contains only linear combinations of $\cosh(\beta C)$ and $\cosh\zeta$. For this purpose, it is helpful to expand the cosines in series and construct the following compositions of interest:

$$\cosh(\sqrt{(\beta C)^2+\zeta^2}) = \cosh\beta C + \cosh\zeta - 1 + \left\{\frac{a_4}{4!}+\frac{a_6}{6!}+\frac{a_8}{8!}+...\right\}, \qquad (2.3)$$

$$\cosh\beta C\cosh\zeta = \cosh\beta C + \cosh\zeta - 1 + \left\{\kappa_4\frac{a_4}{4!}+\kappa_6\frac{a_6}{6!}+\kappa_8\frac{a_8}{8!}+...\right\}, \qquad (2.4)$$

where

$$a_4 = 2(\beta C)^2\zeta^2, \qquad a_6 = 2\left[(\beta C)^4\zeta^2+(\beta C)^2\zeta^4\right],$$
$$a_8 = 3(\beta C)^6\zeta^2 + 4(\beta C)^4\zeta^4 + 3(\beta C)^2\zeta^6 \qquad (2.5)$$

and κ_i are fixed numbers. Now we suggest that for every certain parameter C one could introduce such an "effective" value $\kappa(C)$ that satisfies the relation

$$\left\{\kappa_4\frac{a_4}{4!}+\kappa_6\frac{a_6}{6!}+\kappa_8\frac{a_8}{8!}+...\right\} \simeq \kappa(C)\left\{\frac{a_4}{4!}+\frac{a_6}{6!}+\frac{a_8}{8!}+...\right\}. \qquad (2.6)$$

Note that we put κ independent of ζ – the statement justified by the further procedure when the shape of $\kappa(C)$ is established basing on the approximate $\mathcal{I}(\beta)$ obtained after integration over ζ (see below). So, combining (2.3), (2.4) and (2.6), we have

$$\cosh C + \cosh\sqrt{(\beta C)^2+\zeta^2} \simeq A + B\cosh\zeta, \qquad (2.7)$$

where

$$A(\beta) = \cosh C + \frac{\kappa-1}{\kappa}\left[\cosh\beta C - 1\right], \qquad B(\beta) = \frac{1}{\kappa}\left[\cosh\beta C + \kappa - 1\right]. \qquad (2.8)$$

Substituting (2.7) into (2.2), one gets (when $A^2 > B^2$) [8]

$$\mathcal{I}(\beta) \simeq \frac{1}{C}\int_0^\infty \frac{\sinh C\, d\zeta}{A(\beta)+B(\beta)\cosh\zeta} = \frac{1}{C}\frac{\sinh C}{\sqrt{A^2-B^2}}\ln\frac{A+B+\sqrt{A^2-B^2}}{A+B-\sqrt{A^2-B^2}}. \qquad (2.9)$$

It is seen that at the impact parameter b=0 or β=0, when $A(0)+B(0) = \cosh C + 1 = 2\cosh^2(C/2)$ and $A(0)-B(0) = \cosh C - 1 = 2\sinh^2(C/2)$, one obtains from (2.9) that $\mathcal{I}(0) = 1$, the exact result following directly from (2.2) [8].

For further applications, the integral of interest $\mathcal{I}(\beta)$ has numerically been calculated by (2.2) for the set of $C(= R/a)$ in the region $5 \le C \le 20$ which covers the wide range of changing of physical parameters R and a. Then, the obtained results for $\mathcal{I}(\beta)$ at every C were adjusted to those calculated with the help of the approximate formula (2.9) by using the best fit method to get $\kappa(C)$. It occurs that $\kappa(5) = 15.2$, $\kappa(20)$=511.4 and for intermediate values of C the function $\kappa(C)$ can be represented by the three-parameter expression

$$\log\kappa = 0.47909 + 0.15025\ C - 0.001938\ C^2. \qquad (2.10)$$

Also, for simple quantitative estimations, one can use the "average" kappa adjusted by the two-parameter formula

$$\log\bar{\kappa} = 0.6728 + 0.1018\ C. \qquad (2.11)$$

The results of fitting $\kappa(C)$ are exhibited in Fig.1(a) where the best fit data are represented by stars, the solid line is its three-parameter approximation (2.10) and the dashed one is the two-parameter (2.11).

For a further discussion we transform eq.(2.9) into a more expressive form. To this end, we use the relations

$$A + B = L, \quad A - B = L - y, \qquad (2.12)$$

where

$$L = \cosh C + \cosh\beta C, \quad y = \frac{2}{\kappa}(\cosh\beta C - 1) + 2. \qquad (2.13)$$

Substituting (2.12) and (2.13) into (2.9) and taking L out of the root, one expresses $\mathcal{I}(\beta)$ in the separable form

$$\mathcal{I}(\beta) = \frac{\sinh C}{\cosh C + \cosh\beta C}P(\beta, C) = u_{SF}(\beta)P(\beta, C), \qquad (2.14)$$

where

$$P(\beta, C) = \frac{1}{C}\frac{1}{\sqrt{1-x}}\ln\frac{1+\sqrt{1-x}}{1-\sqrt{1-x}} \qquad (2.15)$$

and

$$x(\beta, C) = \frac{y}{L} = \frac{2}{\kappa}\frac{\cosh\beta C - 1 + \kappa}{\cosh\beta C + \cosh C} = \frac{2}{\kappa}\frac{1}{1+\dfrac{\cosh C}{\cosh\beta C}}\left\{1 + \frac{\kappa-1}{\cosh\beta C}\right\}. \qquad (2.16)$$

Further simplifications can be carried out taking account of $\cosh C \gg \kappa \gg 1$ which follows $x \ll 1$; namely,

$$x(\beta = 0, C) \simeq \frac{2}{\cosh C}, \quad x(\beta = 1, C) \simeq \frac{1}{\kappa}, \quad x(\beta \gg 1, C) \simeq \frac{2}{\kappa}. \qquad (2.17)$$

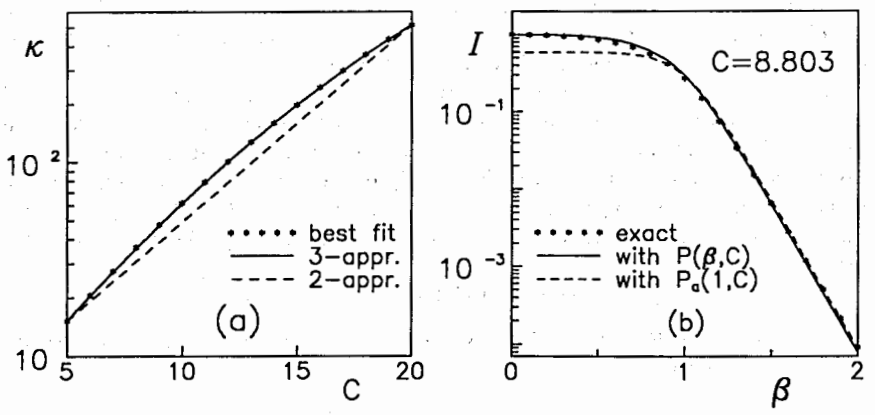

Figure 1: *(a). The best fitted $\kappa(C)$ (stars) and its parametrization by eq.(2.10) (solid line); the straight dashed line is by eq.(2.11). (b). The profile integral (2.2) for the SF-distribution function, computed numerically (stars), and by its approximation (2.14) with $P(\beta, C)$ from (2.15) (solid line) and with $P_a(1, C)$ from ((2.19).*

So, expanding P in (2.15) as a function of x in small x, one obtains

$$P(\beta, C) \simeq \frac{1}{C}[\ln 4 - \ln x]. \tag{2.18}$$

Then, suggesting that the main contribution to elastic scattering is caused (at least for the nucleus-nucleus scattering) by the nuclear surface region $b \simeq R$ or $\beta \simeq 1$, where $x \simeq \kappa^{-1}$, one obtains from (2.18) with the help of (2.10) the approximate expression

$$P_a(1, C) \simeq \frac{1}{C}[\ln 4\kappa] = \frac{1}{C}\left[2.489453 + 0.34597\ C - 0.0046\ C^2\right]. \tag{2.19}$$

The respective nuclear eikonal phase (1.3)

$$\Phi_{N,a}(b) = -\frac{2RU_0}{\hbar v}\frac{\sinh(R/a)}{\cosh(R/a) + \cosh(b/a)} P_a(1, \frac{R}{a}) \tag{2.20}$$

depends on the impact parameter b only as the symmetrized Fermi function.

Fig.1(b) shows an example of behaviour of $\mathcal{I}(\beta)$ calculated numerically by (2.2) (stars) and by the analytic expression (2.14): the solid line is with utilizing $P(\beta, C)$ (2.15); and the dashed line, with a simple $P_a(1, C)$ by (2.19). Their practical coincidence is seen at $b > R$, the region of the main contribution to peripheral collisions.

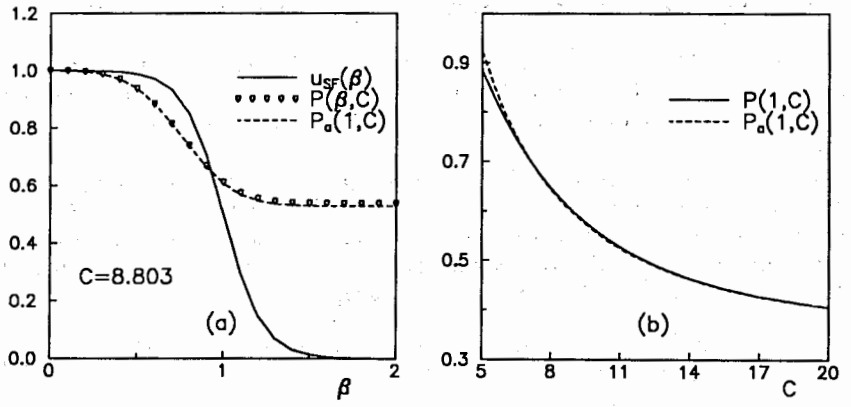

Figure 2: *(a). The symmetrized Fermi function - solid line, the exact gathering functions P - circles, approximate P_a- dashed line. (b). Behaviour of P (solid) and P_a (dashed line) as function of C at $\beta = 1$.*

One should note that the presentation of the phase integral $\mathcal{I}(\beta)$ in the separable form (2.14) makes clear that its main dependence on the impact parameter b is determined by the $u_{SF}(b)$ distribution function which, in fact, is the integrand $u_{SF}(\sqrt{b^2 + z^2})$ of (1.8) taken on the profile sheet at $z = 0$. So, the smooth function $P(\beta, C)$ corrects this dependence, and arises because of different effective lengths $\bar{z}(b)$ of integration over z at every certain b. Thus, it has the meaning of a gathering function which takes account of middle deviation of $u_{SF}(\sqrt{b^2 + z^2})$ from $u_{SF}(b)$ along the path of integration $\bar{z}$.

In Fig.2(a), one can see the behaviour of these two terms, namely, $u_{SF}(b)$ (solid line) and the gathering function P given by the circles for exact $P(\beta, C)$ and by the dashed line for its approximation $P_a(1, C)$. Factors P change less than two times while u_{SF} falls down in orders of its value. A small difference between exact P and approximate P_a functions at $\beta = 1$ is revealed only when $C < 7$, as it is exhibited in Fig.2(b) in dependence of $C = R/a$.

We conclude that if one wants to estimate the profile integrals (2.1) for the realistic Fermi-type distribution functions at given parameters R and a, one should take $\kappa(C)$ at $C = R/a$ from (2.10) and calculate $\mathcal{I}(b)$ with the help of (2.14). Also, for heavy-ion collisions one can use the simple approximate analytic expressions for the gathering function P_a and for the nuclear phase Φ_N which are fully determined by (2.19) and (2.20).

3 Results for elastic scattering and conclusions

In this section, the obtained eikonal phase is applied to methodical calculations of elastic scattering of heavy ions. They are realized for two energies and various atomic numbers of colliding nuclei to cover a wide region of changing of geometrical parameters of nuclear potentials.

In the presence of the Coulomb forces, the Φ_C phases contain the diverged term $\Phi_{pc} = 2\eta \ln(kb) - \Phi_a$ where $\eta = U_B R_c/\hbar c$, $U_B = Z_1 Z_2 e^2/R_c$ and $\Phi_a = 2\eta \ln(2kL)$ with L, being the screening parameter. Therefore, to calculate the amplitude (1.1), one uses a trick by adding and subtracting the scattering amplitude for the point charge potential $U_{pc} = U_B\, u_{pc}(r)$ with $u_{pc} = r/R_c$, as it is obtained in [1]

$$f_{pc}(q) = -ik \int_0^\infty db\, bJ_0(qb)\, e^{i\Phi_{pc}} = -\frac{2k\eta}{q^2}\, e^{-2i\eta \ln(q/2k) + 2i\sigma_0 - i\Phi_a}. \qquad (3.1)$$

Here, $\sigma_0 = \arg\, \Gamma(1+i\eta) \simeq \eta(\ln\eta - 1) + \pi/4$ if $\eta \gg 1$, and $\Phi_a = 2\eta \ln(2kL)$. Then, reproducing the amplitude as $f(q) = f_{pc} + \{f(q) - f_{pc}(q)\}$, one gets

$$f(q) = f_{pc}(q) + ik \int_0^\infty db\, bJ_0(qb)\, e^{i\Phi_{pc}} \left\{1 - e^{i\Phi_N + i\delta\Phi_c}\right\}, \qquad (3.2)$$

where the nuclear phase Φ_N gets the addition $\delta\Phi_c = \Phi_c - \Phi_{pc}$ which does not include the term $\ln(kb)$ at large b, factor $\exp(-i\Phi_a)$ vanishes in the cross section. In practice, for scattering of heavy ions the usually utilized Coulomb potential is that of the uniformly charged ball of radius R_u, and then the δ-term is

$$\delta\Phi_c(b) = \begin{cases} 2\eta\left[\ln(\frac{R_u}{b}) + \ln\left(1 + \sqrt{1 - \frac{b^2}{R_u^2}}\right) - \frac{1}{3}\sqrt{1 - \frac{b^2}{R_u^2}}\left(4 - \frac{b^2}{R_u^2}\right)\right] & b \le R_u \\ 0, & b > R_u. \end{cases} \qquad (3.3)$$

Thus, it is seen that for $b > R_u$, the expression in braces of (3.2) occurs to be $\{1 - \exp(i\Phi_N)\}$ which goes to zero with increasing b.

Fig.3 shows the results of calculations of differential cross sections for elastic scattering of $^{12}C{+}^{24}Mg$, $^{16}O{+}^{120}Sn$, $^{40}Ca{+}^{232}U$ at two energies $E = 30\,A_1\,MeV$ (the left column) and $E = 60\,A_1\,MeV$ (the right column). The parameters of potentials were taken as $V_0 = -50\,MeV$, $W_0 = -20\,MeV$, $R = R_u = 1.1(A_1^{1/3} + A_2^{1/3})\,fm$, $a = 0.65\,fm$. Thus, one has examples for three C=8.756, 12.611 and 16.186. Here we have not included effects of the Coulomb deviation of the straight-ahead trajectory of motion, since they do not change further conclusions. By the same reasons we have not compared our calculations with experimental data.

The high-energy approximation method developed in [1] and [2] for small angles may be applied in the limits of $\theta < \theta_c + \bar{\theta}$, where the classical deflection angle $\theta_c \simeq U_B/E$ is added to expand the standard limitation $\theta < \bar{\theta} = \sqrt{2/kR}$ for (1.1). Then, for the considered collisions we find limits *theta* $< 12°$ for the first example $^{12}C + ^{24}Mg$ at $E = 30\,MeV$/nucleon and $\theta < 9.5°$ at $60\,MeV$/nucleon; also, for the second example with projectiles ^{16}O we have, respectively, 15° and 9.5°; and for the third example with the ^{40}Ca ions, $\theta < 14.5°$ and 8°. Thus, it is seen from Fig.3 that, for the Glauber-Sitenko

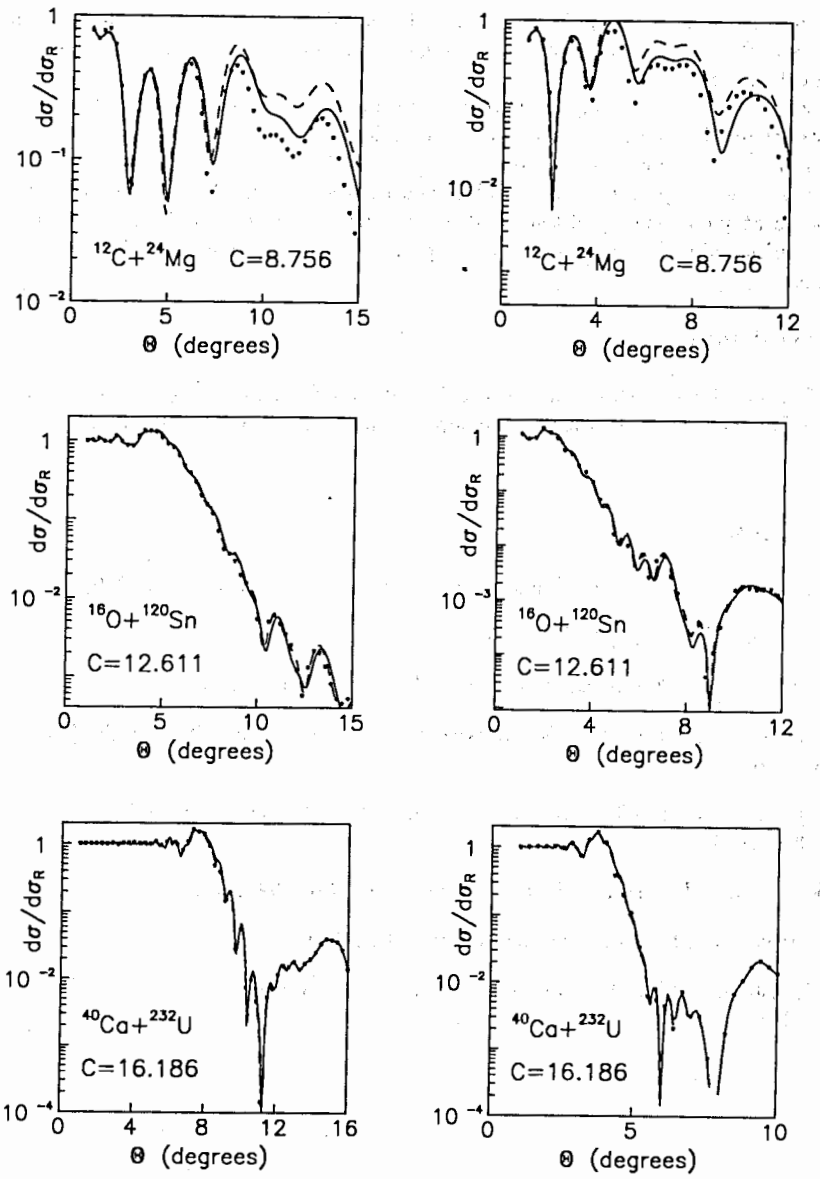

Figure 3: *(a): The heavy ion differential cross sections. The left column is for $E = 30A_1\ MeV$, the right - for $E = 60A_1\ MeV$. Solid lines are exact numerical integration with the profile integral (2.2), dashed lines are when its analytic form (2.14) is used with $P(\beta, C)$, and circles - with approximated $P_a(1, C)$.*

approach in the region of its applicability, all differential cross sections calculated with analytic phases for the SF-type potential are in good agreement with the respective exact numerical calculations.

Then, when utilizing the analytic expressions for phases, calculations occur about two orders faster than with the whole numerical integration.

And the last conclusion is that the analytic eikonal for the symmetrized Fermi distribution of a potential permits one to understand the mechanism of scattering of heavy ions at comparably high energy of tens of MeV per nucleon and, especially, an important role of the peripheral region in forming the structure of diffraction patterns of differential cross sections.

Acknowledgment

One of the authors (V.K.L) thanks the Foundation for Basic Research under the Ministry of Education of Russia for partial support under grant No. 97-40-1.6-6.

References

[1] R.J.Glauber, *in* Lectures on Theor. Phys., **1** (Interscience, New York, 1959);

[2] A.G.Sitenko, Ukr.Fiz.J., **4** (1957) 152.

[3] Yu.N.Eldyshev, V.K.Lukyanov, Yu.S.Pol', Yad.Fiz., **16** (1972) 506.

[4] V.V.Burov, Yu.N.Eldyshev, V.K.Lukyanov, Yu.S.Pol', Preprint E4-8029 (1974), JINR, Dubna.

[5] M.Grypeos, C.Koutroulos, V.Lukyanov, A.Shebeko, J.Phys.G: Nucl. and Part.Phys., **24** (1998) 1913.

[6] D.W.L.Sprung, J.Martorell, J.Phys.A: Math.Gen., **30** (1997) 6525.

[7] J.R.Shepard and E.Rost, Phys.Rev. C, **25** (1982) 2660.

[8] I.S.Gradstein, I.M.Ryzik, Tables of Integrals, Sums, Series and Products, ed. Fiz.-Math., Moscow, 1962.

Received by Publishing Department
on September 27, 1999.